Nanoscale

COMMUNICATION

View Article Online
View Journal | View Issue

Cite this: *Nanoscale*, 2020, **12**, 23959

Received 22nd September 2020,
Accepted 1st November 2020

DOI: 10.1039/d0nr06816k

rsc.li/nanoscale

Spontaneous, solvent-free entrapment of siRNA within lipid nanoparticles†

Jayesh A. Kulkarni, *[a,b,c,d] Sarah B. Thomson, [b] Josh Zaifman,[d,e,f] Jerry Leung,[d] Pamela K. Wagner,[b,c] Austin Hill,[b,c] Yuen Yi C. Tam,[d,e] Pieter R. Cullis, *‡[a,d] Terri L. Petkau[b,c] and Blair R. Leavitt [b,c]

Lipid nanoparticle (LNP) formulations of nucleic acid are leading vaccine candidates for COVID-19, and enabled the first approved RNAi therapeutic, Onpattro. LNPs are composed of ionizable cationic lipids, phosphatidylcholine, cholesterol, and polyethylene glycol (PEG)-lipids, and are produced using rapid-mixing techniques. These procedures involve dissolution of the lipid components in an organic phase and the nucleic acid in an acidic aqueous buffer (pH 4). These solutions are then combined using a continuous mixing device such as a T-mixer or microfluidic device. In this mixing step, particle formation and nucleic acid entrapment occur. Previous work from our group has shown that, in the absence of nucleic acid, the particles formed at pH 4 are vesicular in structure, a portion of these particles are converted to electron-dense structures in the presence of nucleic acid, and the proportion of electron-dense structures increases with nucleic acid content. What remained unclear from previous work was the mechanism by which vesicles form electron-dense structures. In this study, we use cryogenic transmission electron microscopy and dynamic light scattering to show that efficient siRNA entrapment occurs in the absence of ethanol (contrary to the established paradigm), and suggest that nucleic acid entrapment occurs through inversion of preformed vesicles. We also leverage this phenomenon to show that specialized mixers are not required for siRNA entrapment, and that preformed particles at pH 4 can be used for *in vitro* transfection.

Introduction

Lipid nanoparticle (LNP) formulations of nucleic acid have established clinical utility[1] and are the enabling technology of the leading vaccines against SARS-CoV-2 [2] and of Onpattro, the first-ever FDA-approved RNAi therapeutic. These LNPs are composed of ionizable cationic lipids (such as 2,2-dilinoleyl-4-(2-dimethylaminoethyl)-[1,3]-dioxolane (KC2) or dilinoleyl-methyl-4-dimethylaminobutyrate, (MC3)), cholesterol, phosphatidylcholine, and poly-ethylene glycol (PEG) lipids[3–5] and are produced using rapid-mixing techniques where an ethanolic-lipid phase is combined with an acidic aqueous phase containing siRNA.[6–8] The resulting LNP suspension is prepared for administration by buffer-exchange to neutral pH. The rapid-mixing procedure is a bottom-up manufacturing approach that achieves particle formation and nucleic acid entrapment in a single step.[9] The current particle formation paradigm suggests that destabilizing agents (such as ethanol or detergents) are essential for efficient entrapment of siRNA,[6,8,10] and that specialised mixers are required to improve particle homogeneity.[7,11–13]

Recent work using cryo-transmission electron microscopy (cryo-TEM) has shown that rapid-mixing procedures for LNP synthesis generate liposomal structures at pH 4 when produced without nucleic acid.[6,14] However, when produced with siRNA, a combination of electron-dense and liposomal structures are formed (ESI Fig. 1†).[4,6] These observations suggested that the presence of siRNA induces the formation of electron-dense structures, but how this occurred was unclear. Specifically, the question remained of whether the empty vesicles at pH 4 were capable of entrapping siRNA and the role of ethanol in that process. Here we show, using cryo-TEM and

[a]*NanoMedicines Innovation Network, Vancouver, British Columbia, Canada. E-mail: pieterc@mail.ubc.ca, j.kulkarni@alumni.ubc.ca; Fax: +1 (604)-822-4843; Tel: +1 (604)-822-4144*
[b]*Center for Molecular Medicine and Therapeutics, Department of Medical Genetics, University of British Columbia, 950 West 28th Avenue, Vancouver, British Columbia, V5Z 4H4, Canada*
[c]*Incisive Genetics, 301 – 980 George Street, Vancouver, BC, V6A 0H9, Canada*
[d]*Department of Biochemistry and Molecular Biology, University of British Columbia, 2350 Health Sciences Mall, Vancouver, British Columbia, V6T 1Z3, Canada*
[e]*Integrated Nanotherapeutics, 6190 Agronomy Road, Vancouver, BC, V6T 1Z3, Canada*
[f]*Department of Chemistry, University of British Columbia, 2350 Health Sciences Mall, Vancouver, British Columbia, V6T 1Z3, Canada*
†Electronic supplementary information (ESI) available. See DOI: 10.1039/d0nr06816k
‡Present Address: Life Sciences Institute, University of British Columbia, 2350 Health Sciences Mall, Vancouver, British Columbia, V6T 1Z3, Canada

dynamic light scattering, that ethanol is not required for efficient siRNA entrapment, particle formation likely occurs prior to entrapment, and specialized mixers[15] are not required. Based on data presented here and elsewhere, we propose that nucleic acid entrapment at pH 4 occurs through rupture and reformation of positively charged vesicles upon interaction with negatively charged nucleic acid. Finally, we leverage this phenomenon to demonstrate that unloaded vesicles (at pH 4) can be used *in vitro* as functional genomic screening tools.

Results and discussion

Initial studies focused on determining whether vesicles at pH 4 are capable of entrapping nucleic acid, and two types of formulation were prepared. First, we used a process termed *single-phase mixing* (detailed in Fig. 1A). Empty LNPs, composed of 50/10/38.5/1.5 mol% (KC2/DSPC/Chol/PEG-lipid), were combined with pH 4 buffer (without nucleic acid) through a T-junction mixer and dialysed into the same pH 4 buffer to remove solvent, generating *preformed vesicles* (PFV). A second mixing step using the T-mixer combined PFV and siRNA in pH 4 buffer (at amine-to-phosphate (N/P) ratios of 1 and 3), and the resulting systems were dialysed against pH 7.4. Next, a set of particles were prepared using the conventional rapid-mixing approach of combining lipids in organic solvent with siRNA in aqueous pH 4 buffer (termed *two-phase mixing*) followed by dialysis against pH 7.4. Regardless of the procedure used, the resulting particles at N/P 1 and 3 displayed essentially identical morphology, particle size, and entrapment efficiency (Fig. 1B–D). It should also be noted that particles produced using two-phase mixing that are dialysed into pH 4 buffer to remove solvent and subsequently dialysed against pH 7.4 display the same morphology as those where LNPs are dialysed directly against pH 7.4 (ESI Fig. 2†), which suggests that ethanol does not dictate the morphology of these systems. In addition to this, the "intermediate" particles that are formed at pH 4 by both single- and two-phase methods display identical morphology (ESI Fig. 3†). These results suggest that particle formation can be completely decoupled from siRNA entrapment, and the series of events that occurs immediately after rapid mixing (in a two-phase system) likely includes the formation of nucleating vesicles that are "stitched" together (or fused) by siRNA until the negative charges are completely consumed.

If this stitching process occurs, the role of PEG-lipid at pH 4 is important, as we have previously shown that PEG-lipids limit fusion of particles.[14,16] To study this, single-phase mixing was used to combine PFV composed of KC2/DSPC/Chol (50/10/38.5 mol%) with siRNA at N/P = 1 or 3. PEG-lipid was then spiked into an aliquot of each suspension following mixing. In all cases, ethanol was maintained less than 0.1% v/v. The particle sizing data and polydispersity indices of the formulations is shown in Fig. 2. In the absence of PEG-lipid, the particles formed aggregates and heterogenous suspensions (PDI > 0.2), and when PEG-lipid was added post-mixing, N/P = 1 samples were larger and more heterogeneous than their conventionally-produced counterparts. This suggests, for samples prepared at N/P = 1, that PEG-lipid inhibits fusion of the emerging particles at pH 4. Comparatively, for N/P = 3 systems, if PEG-lipid is added post-mixing, the resulting particles are essentially identical to those produced by conventional two-phase methods. The critical observation is that PEG-lipid inhibits fusion of LNP systems at N/P = 1 during the rapid-mixing process, but only acts during pH neutralization for systems at N/P = 3. The latter formulation contains an excess of ionizable

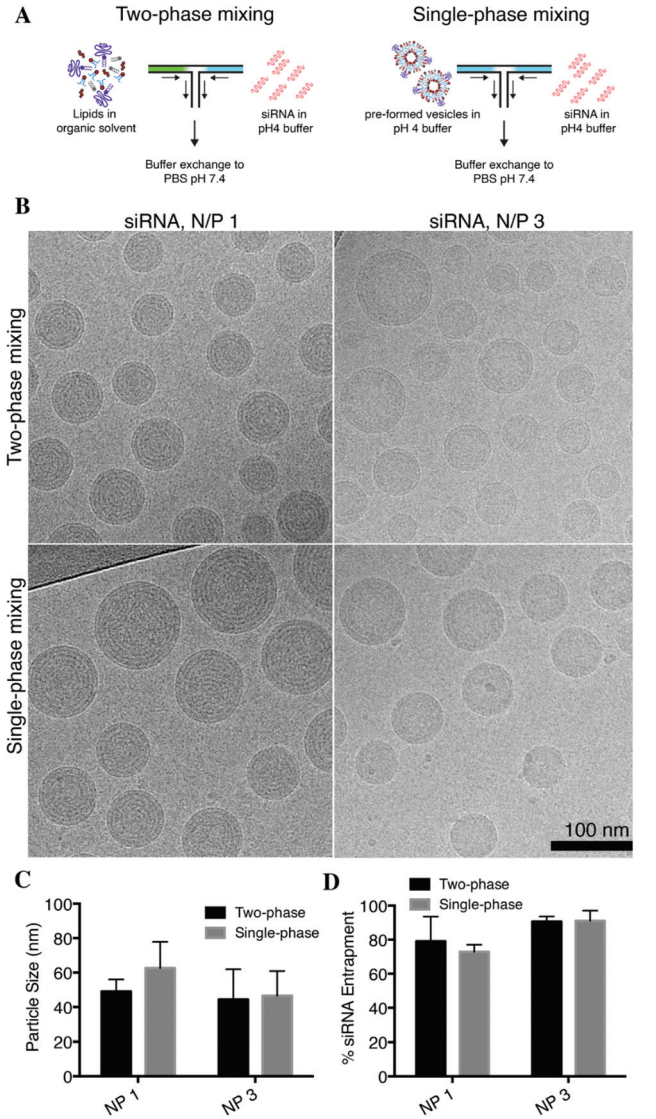

Fig. 1 Single-phase mixing generates LNPs with similar properties as conventional methods of production. LNP-siRNA composed of KC2/DSPC/Chol/PEG-lipid (50/10/38.5/1.5 mol%) were formulated using single-phase or two-phase mixing (A). (B) Representative cryo-TEM images of LNPs produced by single-phase or two-phase at N/P = 1 or 3, imaged after the pH is neutralized. Scale bar = 100 nm. (C) Particle sizing data as measured by DLS. (D) siRNA entrapment as measured by RiboGreen. Results indicate mean ± standard deviation (n = 3) of three independent formulations.

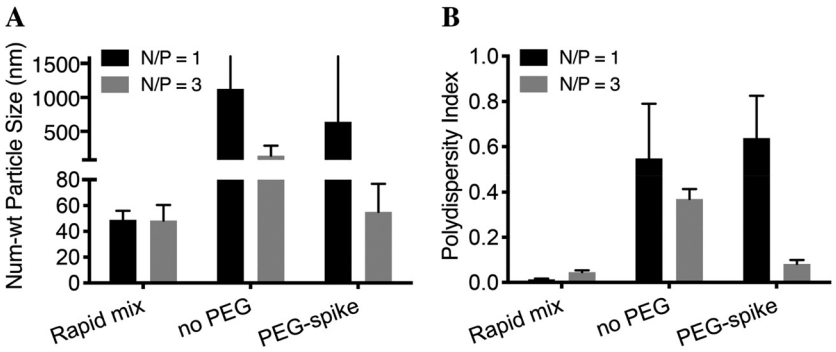

Fig. 2 PEG-lipid inhibits the fusion of N/P = 1 particles immediately after mixing (at pH 4), but only during the neutralization of the pH for N/P = 3 particles. Particle sizing data (A) and associated polydispersity indices as generated by DLS measurements (B). LNP-siRNA formulations composed of KC2/DSPC/Chol/PEG-lipid at 50/10/38.5/1.5 mol% were formulated using two-phase mixing and are labelled as "Rapid mix". The single-phase procedure was applied to LNP formulations composed of KC2/DSPC/Chol at 50/10/38.5 (mol%). These PEG-free preformed vesicles at pH 4 were combined with siRNA at N/P = 1 or 3. In one case (no PEG), the formulation was dialyzed against PBS pH 7.4, and in another case, PEG-lipid corresponding to 1.5 mol% was spiked into the mixture, and then dialyzed to neutralize the pH. Results indicate mean ± standard deviation (n = 3) of three independent formulations.

lipid, and therefore it is expected that at pH 4, the positive charge on the surface of emerging LNPs results in repulsive forces between particles (once all siRNA molecules are entrapped). These findings are also consistent with previous data[6] that suggest LNP-siRNA at N/P = 1 do not change in morphology as the pH is neutralized. Comparatively, LNP-siRNA at N/P = 3 undergo a dramatic increase in particle size (and change in morphology) when the pH is neutralized.[6] In this case, the PEG-lipid has been determined to play a role in limiting the fusion of precursor particles.[14]

In order to further study the interaction between positively charged vesicles and siRNA, PFV composed of KC2/PEG-lipid (98.5/1.5 mol%) were prepared in pH 4 buffer. Using single-phase mixing, the PFV were combined with siRNA at N/P = 1 and 3, and the resulting systems were concentrated and analysed by cryo-TEM (ESI Fig. 4†). In the absence of siRNA, the systems are composed of small unilamellar particles, but in the presence of siRNA at N/P = 1, the particles are converted into stacked lamellar structures (aggregates) with no evidence of liposomal morphology. At N/P = 3, the structures are a mixture of electron dense particles and liposomal structures. The formation of stacked lamellar structures, with no other definitive particle morphology, suggests that siRNA entrapment occurs through the rupture and reorganization of lipids (in the complete absence of solvent).

The results presented here also offer new insights on the mechanism by which entrapment of siRNA occurs in LNP formulations. First, the data strongly suggests that the process of rapid mixing involves the formation of vesicles prior to interaction with siRNA. Specifically, the dilution of lipidic-ethanol into the aqueous phase results in the formation of nucleating vesicles, which subsequently entrap siRNA. Next, the data shows that these processes can be entirely separated, with particle formation (and solvent removal) occurring prior to entrapment. Based on these findings and previous work,[6,8,17] a potential mechanism of nucleic acid encapsulation is detailed in Fig. 3. The very first events that occur following dilution of lipids into the aqueous phase is the formation of positively charged vesicles. Subsequently, these vesicles are decorated with polyanionic molecules that act as a zipper between multiple membrane surfaces. As the region of nucleic acid-membrane contact increases, the vesicles flatten against each other, resulting in localized regions of high strain. This heightened energy state (strain) is dissipated through membrane rupture and reformation[17] into "planarized" stacked membranes[18] observed as multilamellar structures. Substantial previous work[7,8,11,15,19] had suggested that these processes only occurred in the presence of ethanol, however, we have shown here that LNP systems composed of these ionizable cationic lipids undergo such reorganisation in the absence of ethanol.

The possibility of leveraging this mechanism for functional genomic screening to support LNP-enabled personalized medicine approaches became readily apparent. For example, PFV systems can be combined with a specific nucleic acid sequence for functional testing in patient-derived primary cells which are often susceptible to the toxic effects of transfection reagents. A current limitation of LNP production is that substantial amounts of material (~100–300 μg of nucleic acid) are required by rapid-mixing processes to account for dead-volumes within mixers, and to ensure efficient mixing occurs. Formulations produced using the typical two-phase approach also contain organic solvent (ethanol), which requires a buffer-exchange step for removal. Given the data described in this study, we postulated that PFV could be formed at pH 4, stored, and combined with nucleic acid on the benchtop immediately before cell treatment in the absence of any specialized mixers or equipment.[15] This would also dramatically reduce the amount of material required to only the quantity necessary for a regulatory response (potentially < 1 μg).

To test this, we assessed the functionality of PFV systems compared to counterparts produced by rapid-mixing in dividing cell culture using a 22Rv1-luciferase cell line. Preformed

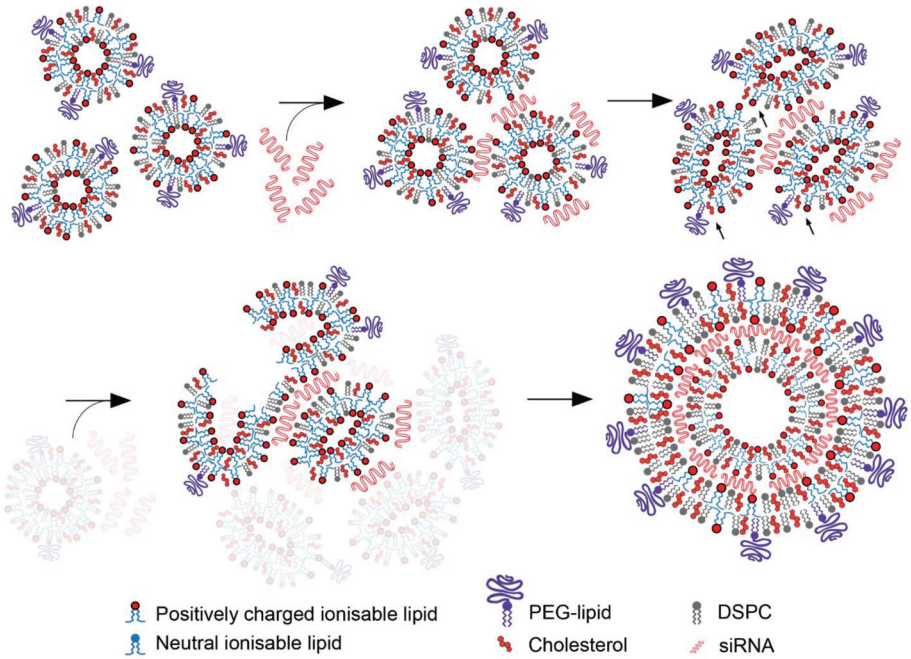

Fig. 3 Proposed mechanism of siRNA entrapment and formation of siRNA-lipid bilayers following rapid-mixing (at pH 4). Following rapid-mixing and upon dilution of the ethanolic-lipid phase into the aqueous phase, it is proposed the very initial events lead to formation of positively charged bilayer structures (top left). Subsequently, interactions with siRNA lead to controlled vesicle aggregation (top middle). Complete association of the siRNA molecules with regions of the lipid membrane lead to substantial destabilization of the bilayer as the vesicles are quite small, and such deformations can have a pronounced impact on membrane integrity (top left). Regions of extreme membrane curvature with decreased lipid coverage (black arrows, top right) are likely points at which particle rupture occurs (bottom left) until almost all of the negative charges have been consumed (bottom right). It should be noted that while only a limited number of vesicles are depicted in two dimensions, calculations suggest almost 36 vesicles fuse to form a single particle which almost definitely occurs in all three dimensions. This has been pictorially described at the bottom left with translucent components. For N/P = 1 formulations, this results in a series of concentric rings or multi-lamellar structures. Our results suggest that at pH 4, this fusion is limited by the PEG-lipid. For N/P = 3 formulations, the stitching of vesicles is likely limited by charge repulsion once all negative charges are consumed. Additionally, the excess of lipid results in systems that are not always concentric rings, but potentially stacked membranes with bilayer protrusions from the surface of the particles. Such systems have been imaged previously using high resolution cryo-TEM.[6] Particles not interacting with siRNA retain their bilayer structure until the pH of the buffer is neutralized whence the final LNP-siRNA particles are formed.

vesicles composed of KC2, DSPC, cholesterol, and PEG-lipid (50/10/38.5/1.5 mol%) were combined with siRNA against firefly luciferase (PFV-siLuc) and incubated for at least 10 minutes prior to use. LNPs prepared by single- and two-phase mixing displayed identical transfection profiles, but PFV systems required higher doses to achieve the same level of gene silencing (Fig. 4A). It should be noted that in this procedure, PFV systems are combined with nucleic acid at pH 4 and therefore particle formation is only complete upon dilution of the pH 4 buffer with complete cell growth medium. This finding is consistent with the requirement of pH neutralization to complete particle formation,[6,14] and the potential for serum proteins in media supplements (FBS) to interfere with complete LNP formation. To investigate the latter possibility, we studied the ability of PFV-siRNA systems to modulate gene expression in neurons *in vitro*. Primary cortical neurons, which are maintained in serum-free medium, were isolated from transgenic GFP-expressing mice and, at day *in vitro* (DIV) 7, were treated with PFV-siRNA against GFP (Fig. 4B). PFV-siRNA treatments were performed using medium supplemented with ApoE which is required for LNP activity with cells cultured in medium lacking serum.[20] Impressively, PFV systems displayed an essentially equivalent level of transfection as LNPs generated using both single- and two-phase approaches. There was no indication of toxicity associated with PFV-siRNA treatment (ESI Fig. 5†), consistent with previous reports of conventionally-prepared LNP-siRNA being well-tolerated by neurons.[20]

Finally, we evaluated the utility of PFV-siRNA systems for functional genomic screening applications by testing four different monovalent ionizable lipids with a range of *in vivo* gene-silencing potencies.[4] MC3 was chosen because it is considered the gold-standard for siRNA delivery,[1,4] DLinDAP and DODAP as they have poor transfection competencies,[21] and DODMA was included as the non-biodegradable analogue of DODAP. All formulations (including a control two-phase LNP) displayed high entrapment efficiencies (ESI Fig. 6A†). Neurons in culture were treated with siRNA against the murine analogue of huntingtin (*Htt*) combined with MC3-LNP (two-phase) or PFV composed of the aforementioned ionizable lipids. Cells treated with si*Htt* displayed ~60% knockdown with MC3- and DODMA-PFV, ~35% with DLinDAP-PFV, and no knockdown

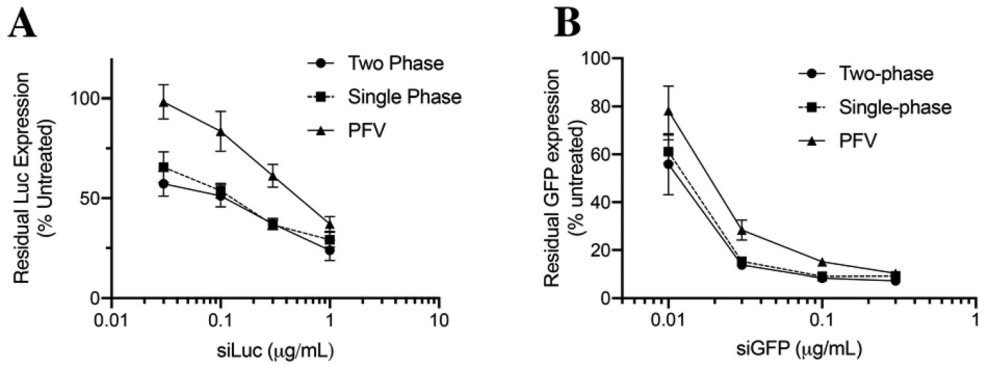

Fig. 4 PFV at pH 4 display utility for transfection procedures *in vitro*. LNPs composed of KC2/DSPC/Chol/PEG-lipid (50/10/38.5/1.5 mol%) were prepared with siRNA using the conventional two-phase or single-phase approach. PFV were prepared with the same composition and stored at pH 4. (A) 22Rv1 cells stably expressing luciferase were treated with LNP or PFV systems at various doses, and luciferase expression measured 24 hours later. (B) Knockdown of GFP in primary cortical neurons from transgenic-GFP mice, measured by qPCR 72 hours following treatment. Results indicate mean ± standard deviation of three independent biological replicates.

with DODAP-PFV (ESI Fig. 6B†). At the highest dose of siRNA tested, an off-target siRNA sequence (siLuc) and ApoE alone as negative controls did not induce *Htt* knockdown (ESI Fig. 6C†). This finding is consistent with previous data[21] that suggests DAP-lipids are poor transfection reagents, while DMA-containing lipids are less susceptible to hydrolysis and are more stable following uptake into target cells (structures in ESI Fig. 7†).

Conclusion

Overall, the results presented here provide insight into a number of previously uncharacterized aspects of LNP technology. First and foremost, we showed that siRNA encapsulation within LNPs does not require ethanol. Second, we showed that particle formation can be decoupled from encapsulation of nucleic acid. Next, we proposed a model by which nucleic acid entrapment occurs that is consistent with previous hypotheses. We suggest that preformed vesicles initially interact with siRNA which promotes destabilization of the membrane and fusion of particles whereby the siRNA becomes internalized. Finally, we leverage this phenomenon to demonstrate the utility of PFV systems as functional genomic tools with relevance to personalized medicine and with potential application for the development of *ex vivo* gene therapies. The results indicate that the techniques described here can allow for a >100-fold reduction in material requirements in a manner that does not require specialized instrumentation.

Materials and methods

Materials

The lipids 1,2-distearoyl-*sn-glycero*-3-phosphocholine (DSPC), and 1,2-distearoyl-*sn-glycero*-3-phosphoethanolamine-*N*-[methoxy(polyethylene glycol)-2000] (ammonium salt) (PEG-DSPE) were purchased from Avanti Polar Lipids (Alabaster, AL). The ionizable amino-lipid 2,2-dilinoleyl-4-(2-dimethylaminoethyl)-[1,3]-dioxolane (KC2) was synthesized by Biofine International (Vancouver, BC). Cholesterol was purchased from Sigma-Aldrich (St Louis, MO). Heptatriaconta-6,9,28,31-tetraen-19-yl-4-(dimethylamino)butanoate (MC3)[22] and (*R*)-2,3-bis(tetradecyloxy)propyl-1-(methoxy polyethylene glycol 2000) carbamate (PEG-DMG) was synthesized as previously described.[23] TEM grids were purchased from Ted Pella, Inc. (Redding, CA). Transgenic GFP-expressing C57BL/6J mice were a generous gift from Dr Colin Ross. C57BL/6J mice (JAX #000664) were purchased from The Jackson Laboratory (Bar Harbor, ME). Hibernate™E medium was purchased from BrainBits LLC (Springfield, IL). All other cell culture and quantitative RT-PCR reagents were purchased from Life Technologies (Burlington, ON). Quantitative RT-PCR primers and siRNAs against firefly luciferase[24] and green fluorescent protein[25] were purchased from Integrated DNA Technologies (Coralville, IA). siRNA against murine *Htt* was purchased from Ambion (*Silencer® Select Pre-designed siRNA*, Invitrogen, Carlsbad, CA). All lipids used in this study are shown in ESI Fig. 7.†

Preparation of empty LNP

LNP were prepared as previously described.[6,14,26] Briefly, lipid components (KC2, Chol, DSPC, and PEG-lipid) at appropriate ratios were dissolved in ethanol to a concentration of 20 mM total lipid. The aqueous phase consisted of 25 mM sodium acetate pH 4 (or pH 4 buffer). The two solutions were mixed through a T-junction mixer[27,28] at a total flow rate of 20 mL min^{-1}, and a flow rate ratio of 3 : 1 v/v (corresponding to 15 : 5 mL min^{-1} aqueous : organic phase). The resulting suspension was subsequently dialyzed against 1000-fold volume of the same sodium acetate pH 4 buffer or against phosphate buffered saline (PBS pH 7.4).

Preparation of LNP containing nucleic acid

Two-phase mixing. LNP-nucleic acid were prepared as previously described.[6,14,26] Briefly, lipid components (ionizable lipid, Chol, DSPC, and PEG-lipid) at appropriate ratios were

dissolved in ethanol to a concentration of 10 mM total lipid. Purified nucleic acid polymers were dissolved in 25 mM sodium acetate pH 4 buffer to achieve the desired N/P ratio. The two solutions were mixed through a T-junction mixer[27,28] at a total flow rate of 20 mL min^{-1}, and a flow rate ratio of 3 : 1 v/v (aqueous : organic phase). The resulting suspension was subsequently dialyzed against the same acetate buffer, or directly against PBS pH 7.4.

Single-phase mixing. Empty LNPs (compositions in main text) at pH 4 without ethanol were concentrated to 10 mM total lipid. As above, nucleic acids were dissolved in 25 mM sodium acetate pH 4 buffer to achieve the desired N/P ratio. A second T-junction[27,28] mixing step was used to combine the preformed vesicles with the nucleic acid at a total flow rate of 20 mL min^{-1}, and a flow rate ratio of 3 : 1 v/v (nucleic acid : PFV). The resulting suspension was subsequently dialyzed against PBS pH 7.4 overnight.

Following dialysis, PFV or LNPs were concentrated using Amicon centrifugal filtration units (Millipore Sigma, Burlington, MA) with a 10 kDa NMWCO.

Mice

Mice were housed on ventilated racks in a specific pathogen-free barrier facility under a 12 h light/dark cycle. Prior to breeding, mice were group-housed with their littermates to a maximum of five mice per cage and given free access to food and water. To generate embryos for primary neuronal culture, male and female mice of appropriate ages were paired in clean single cages. Breeding pairs were separated immediately following the detection of a seminal plug in the vaginal canal, and pregnant female mice were single housed until collection. All animal work was carried out with the approval of the Canadian Council for Animal Care and the University of British Columbia's Animal Care Committee.

22Rv1 cell culture

22Rv1 cells stably expressing Luciferase were cultured in RPMI 1640 with 10% FBS. Cells were plated at a density of 8000 cells per well in 96-well plates and allowed to adhere for 24 hours. Additional details below.

Primary cell culture

Primary cortical neuron cultures were derived from transgenic GFP-expressing C57BL/6J mice or wild-type C57BL/6J mice at embryonic day 17.5. Cortices were isolated by dissection in ice-cold HBSS (Gibco) and collected in Hibernate™ E medium (BrainBits LLC) supplemented with 0.5 mM L-glutamine (Hyclone). Tissue was digested in a 0.05% (v/v) trypsin (Hyclone) solution in a 37 °C water bath for 15 minutes. Following trypsin inactivation by FBS addition (Hyclone), digested tissue was dissociated by trituration using a constrained 5 mL serological pipette and filtered through a 40 μM cell strainer (Falcon). Filtered cells were pelleted by centrifugation for 5 minutes at 800 rpm, washed once with HBSS to remove FBS, and resuspended in warmed Neurobasal medium (Gibco) supplemented with 2% (v/v) 50× B27 (Gibco), 0.5 mM L-glutamine (Hyclone), and 0.5 mg mL^{-1} penicillin/streptomycin (Hyclone). Neurons were plated in poly-D-lysine-coated 24-well and 96-well plates (Falcon; Corning) at a density of 1.5×10^5 cells per mL and maintained in a humidified atmosphere at 37 °C and 5% CO_2.

PFV-siRNA transfection

All reagents were mixed on the benchtop. PFV were combined with siRNA at a ratio of 0.058 μg siRNA per μmole lipid. Lipid solutions were mixed with siRNA briefly by pipette and incubated at room temperature for 10 minutes.

Neurons. Neurobasal medium (Gibco) supplemented with 1 μg mL^{-1} recombinant human ApoE4 (PeproTech) was added to dilute the PFV-siRNA solution which is required for transfection.[20] To treat neurons, 50% of the plating medium was removed from each well and replaced with an equivalent volume of PFV-siRNA solution in medium. The reported siRNA doses are representative of the final concentration in the well. Primary neuronal cells were maintained *in vitro* for seven days (DIV7) prior to PFV-siRNA transfection.

22Rv1-Luc cells. 100% of the plating medium was removed from each well and replaced with an equivalent volume of diluted PFV-siRNA solution. LNP- or PFV-siRNA were diluted into complete medium at 0.03–1.0 μg mL^{-1} siRNA. The luciferase assay (Steady-Glo Luciferase kit, Promega, Madison, WI) was performed 24 hours post-treatment.

Neuronal viability assay

The viability of PFV-treated primary cortical neurons was assessed 72 h post-transfection (DIV10) using the CellTiter-Glo® luminescent cell viability assay system (Promega) according to the manufacturer's instructions. Briefly, neuronal plating/treatment medium was replaced with warmed Neurobasal-A, equilibrated to room temperature, and combined with an equivalent volume of CellTiter-Glo® reagent. Cells were lysed by mixing on an orbital shaker for two minutes and incubated on the benchtop for an additional 10 minutes. Luminescence was quantified using a POLARstar Omega plate reader (BMG LABTECH). Values are presented as % control and represent $n = 4$ wells per condition.

Quantitative RT-PCR

Primary cortical neurons in 24-well plates were collected for RNA extraction by washing with 1× PBS (Gibco), scraping in 700 μL lysis buffer (Invitrogen) containing 1% 2-mercaptoethanol, and freezing on dry ice. Total RNA was extracted from thawed samples using the PureLink® RNA Mini kit (Invitrogen) according to the manufacturer's instructions. PureLink DNase (Invitrogen) was used to degrade residual genomic DNA on preparation columns to increase RNA yield and purity. RNA concentrations were measured using a Nanodrop 2000 spectrophotometer (Thermo Scientific). Reverse transcription was performed using the SuperScript® VILO™ cDNA Synthesis Kit (Invitrogen). Amplification of cDNA was performed using FastSYBR® green master mix (Applied Biosystems) and the StepOne Plus Real-Time PCR

Table 1 RT-qPCR primer sequences

Target	Forward (5′ → 3′)	Reverse (5′ → 3′)
eGFP	CAGAAGAACGGCATCAAGG	ACGAACTCCAGCAGGACCAT
Htt	TGGTAATGACAGTTGAGGCCC	CCAGGTTGTACTGCAATGGCT
Csnk2a2	CCACATAGACCTAGATCCACACTTCA	AGGTGCCTGTTCTCACTATGGATAA
ActB	CCAGCCTTCCTTCTTGGGTAT	TGTGTTGGCATAGAGGTCTTTACG

System (Applied Biosystems). All samples were run in duplicate. mRNA levels were quantified by standard curve using 10-fold serial dilutions of a portion of untreated control samples. Relative quantities of target mRNA were calculated as the ratio between target mRNA abundance and a normalization factor created using two control genes (*Csnk2a2* and *ActB*) based on GeNorm.[29] Values are presented as % control and represent n = 3–4 wells per condition. Primer sequences are provided in Table 1.

Cryogenic transmission electron microscopy (cryo-TEM)

Cryo-TEM was performed as previously described.[6] Briefly, concentrated LNP suspensions (20–25 mg mL^{-1} of total lipid) were added to glow-discharged copper grids, plunge-frozen using a FEI Mark IV Vitrobot (FEI, Hillsboro, OR), and stored in liquid nitrogen. A FEI LaB6 G2 TEM (FEI, Hillsboro, OR) was used to image all samples. The instrument was operated at 200 kV under low-dose conditions. A bottom-mount FEI Eagle 4 K CCD camera was used to capture all images. All samples (unless otherwise stated) were imaged at a 47k–62k magnification with a nominal under-focus of 1–2 μm to enhance contrast. Sample preparation and imaging was performed at the UBC Bioimaging Facility (Vancouver, BC).

Analysis of LNP

Cryo-TEM micrographs obtained for each sample were characterized for particle size (as compared by length to the scale bar), performed by manual counting 200 LNPs to account for scattering interference (with DLS) from different particle morphologies. This technique has been shown to closely correlate with the number-weighted average produced by dynamic light scattering.[7,30] Similarly, the proportion of LNPs in the dumbbell or bilamellar morphology was determined manually. Lipid concentrations were measured using the Cholesterol E Total-Cholesterol assay (Wako Diagnostics, Richmond, VA). RNA entrapment was measured using the procedure described elsewhere.[31]

Conflicts of interest

JAK, TLP, AH, PKW, and BRL have financial interest in Incisive Genetics. BRL is CEO and co-Founder of Incisive Genetics Inc. JAK, TLP, AH and PKW are co-Founders of Incisive Genetics Inc.

BRL, JAK, TLP, PRC, AH, and PKW with the University of British Columbia have filed a patent application on the compositions and methods in this work (PCT/US2019/055472).

Incisive Genetics Inc. has licensed this intellectual property from The University of British Columbia.

Acknowledgements

JAK and PRC are funded by Foundation grant (FDN 148469) from the Canadian Institutes of Health Research, and a British Columbia Innovation Council Ignite grant. JAK is supported (in part) by a postdoctoral fellowship from NanoMedicines Innovation Network (NMIN), a member of the Networks of Centers of Excellence Canada program. SBT is supported by a doctoral fellowship from the Huntington Society of Canada (#10901). BRL is funded (in part) by a project grant from NMIN (PID#:2019-T2-03). PRC is the scientific director and awardee of NMIN. The authors would like to thank Dr Norbert Maurer (Evonik Canada Inc) for helpful discussions.

References

1 A. Akinc, M. A. Maier, M. Manoharan, K. Fitzgerald, M. Jayaraman, S. Barros, S. Ansell, X. Du, M. J. Hope, T. D. Madden, B. L. Mui, S. C. Semple, Y. K. Tam, M. Ciufolini, D. Witzigmann, J. A. Kulkarni, R. van der Meel and P. R. Cullis, *Nat. Nanotechnol.*, 2019, **14**, 1084–1087.
2 M. Therapeutics, 2020, https://investors.modernatx.com/news-releases/news-release-details/moderna-ships-mrna-vaccine-against-novel-coronavirus-mrna-1273.
3 P. R. Cullis and M. J. Hope, *Molecular therapy : the journal of the American Society of Gene Therapy*, 2017, pp. 1467–1475.
4 J. A. Kulkarni, D. Witzigmann, S. Chen, P. R. Cullis and R. van der Meel, *Acc. Chem. Res.*, 2019, **52**(9), 2435–2444.
5 J. A. Kulkarni, P. R. Cullis and R. van der Meel, *Nucleic Acid Ther.*, 2018, **28**, 146–157.
6 J. A. Kulkarni, M. M. Darjuan, J. E. Mercer, S. Chen, R. van der Meel, J. L. Thewalt, Y. Y. C. Tam and P. R. Cullis, *ACS Nano*, 2018, **12**, 4787–4795.
7 A. K. Leung, I. M. Hafez, S. Baoukina, N. M. Belliveau, I. V. Zhigaltsev, E. Afshinmanesh, D. P. Tieleman, C. L. Hansen, M. J. Hope and P. R. Cullis, *J. Phys. Chem. C*, 2012, **116**, 18440–18450.
8 N. Maurer, K. F. Wong, H. Stark, L. Louie, D. McIntosh, T. Wong, P. Scherrer, S. C. Semple and P. R. Cullis, *Biophys. J.*, 2001, **80**, 2310–2326.
9 M. J. W. Evers, J. A. Kulkarni, R. der Meel, P. R. Cullis, P. Vader and R. M. Schiffelers, *Small Methods*, 2018, **2**, 1700375.

10 J. J. Wheeler, L. Palmer, M. Ossanlou, I. MacLachlan, R. W. Graham, Y. P. Zhang, M. J. Hope, P. Scherrer and P. R. Cullis, *Gene Ther.*, 1999, **6**, 271–281.
11 N. M. Belliveau, J. Huft, P. J. Lin, S. Chen, A. K. Leung, T. J. Leaver, A. W. Wild, J. B. Lee, R. J. Taylor, Y. K. Tam, C. L. Hansen and P. R. Cullis, *Mol. Ther.–Nucleic Acids*, 2012, **1**(8), e37.
12 A. K. Leung, Y. Y. Tam, S. Chen, I. M. Hafez and P. R. Cullis, *J. Phys. Chem. B*, 2015, **119**, 8698–8706.
13 P. N. Inc, Precision NanoSystems Inc., https://www.precisionnanosystems.com/, (accessed 16 July 2019).
14 J. A. Kulkarni, D. Witzigmann, J. Leung, R. van der Meel, J. Zaifman, M. M. Darjuan, H. M. Grisch-Chan, B. Thöny, Y. Y. C. Tam and P. R. Cullis, *Nanoscale*, 2019, **11**(18), 9023–9031.
15 A. Thomas, S. M. Garg, R. A. G. De Souza, E. Ouellet, G. Tharmarajah, D. Reichert, M. Ordobadi, S. Ip and E. C. Ramsay, *Methods Mol. Biol.*, 2018, **1792**, 193–203.
16 J. A. Kulkarni, D. Witzigmann, J. Leung, Y. Y. C. Tam and P. R. Cullis, *Nanoscale*, 2019, **11**, 21733–21739.
17 E. A. Evans and V. A. Parsegian, *Ann. N. Y. Acad. Sci.*, 1983, **416**, 13–33.
18 S. Huebner, B. J. Battersby, R. Grimm and G. Cevc, *Biophys. J.*, 1999, **76**, 3158–3166.
19 M. E. Gindy, K. DiFelice, V. Kumar, R. K. Prud'homme, R. Celano, R. M. Haas, J. S. Smith and D. Boardman, *Langmuir*, 2014, **30**, 4613–4622.
20 R. L. Rungta, H. B. Choi, P. J. Lin, R. W. Ko, D. Ashby, J. Nair, M. Manoharan, P. R. Cullis and B. A. Macvicar, *Mol. Ther.–Nucleic Acids*, 2013, **2**, e136.
21 P. J. Lin, Y. Y. Tam, I. Hafez, A. Sandhu, S. Chen, M. A. Ciufolini, I. R. Nabi and P. R. Cullis, *Nanomedicine*, 2013, **9**, 233–246.
22 M. Jayaraman, S. M. Ansell, B. L. Mui, Y. K. Tam, J. Chen, X. Du, D. Butler, L. Eltepu, S. Matsuda, J. K. Narayanannair, K. G. Rajeev, I. M. Hafez, A. Akinc, M. A. Maier, M. A. Tracy, P. R. Cullis, T. D. Madden, M. Manoharan and M. J. Hope, *Angew. Chem., Int. Ed.*, 2012, **51**, 8529–8533.
23 A. Akinc, A. Zumbuehl, M. Goldberg, E. S. Leshchiner, V. Busini, N. Hossain, S. A. Bacallado, D. N. Nguyen, J. Fuller, R. Alvarez, A. Borodovsky, T. Borland, R. Constien, A. de Fougerolles, J. R. Dorkin, K. Narayanannair Jayaprakash, M. Jayaraman, M. John, V. Koteliansky, M. Manoharan, L. Nechev, J. Qin, T. Racie, D. Raitcheva, K. G. Rajeev, D. W. Sah, J. Soutschek, I. Toudjarska, H. P. Vornlocher, T. S. Zimmermann, R. Langer and D. G. Anderson, *Nat. Biotechnol.*, 2008, **26**, 561–569.
24 G. Basha, M. Ordobadi, W. R. Scott, A. Cottle, Y. Liu, H. Wang and P. R. Cullis, *Mol. Ther.–Nucleic Acids*, 2016, **5**, e363.
25 Y. Yamamoto, P. J. Lin, E. Beraldi, F. Zhang, Y. Kawai, J. Leong, H. Katsumi, L. Fazli, R. Fraser, P. R. Cullis and M. Gleave, *Clin. Cancer Res.*, 2015, **21**, 4845–4855.
26 J. A. Kulkarni, J. L. Myhre, S. Chen, Y. Y. C. Tam, A. Danescu, J. M. Richman and P. R. Cullis, *Nanomedicine*, 2016, **13**, 1377–1387.
27 S. Hirota, C. T. de Ilarduya, L. G. Barron and F. C. Szoka Jr., *BioTechniques*, 1999, **27**, 286–290.
28 J. A. Kulkarni, Y. Y. C. Tam, S. Chen, Y. K. Tam, J. Zaifman, P. R. Cullis and S. Biswas, *Nanoscale*, 2017, **9**, 13600–13609.
29 J. Vandesompele, K. De Preter, F. Pattyn, B. Poppe, N. Van Roy, A. De Paepe and F. Speleman, *Genome Biol.*, 2002, **3**, research0034.1, DOI: 10.1186/gb-2002-3-7-research0034.
30 S. Chen, Y. Y. Tam, P. J. Lin, A. K. Leung, Y. K. Tam and P. R. Cullis, *J. Controlled Release*, 2014, **196**, 106–112.
31 S. Chen, Y. Y. Tam, P. J. Lin, M. M. Sung, Y. K. Tam and P. R. Cullis, *J. Controlled Release*, 2016, **235**, 236–244.